

LA-UR-

09-04091

Approved for public release;
distribution is unlimited.

Title: Ice formation in PEM Fuel Cells Operated Isothermally at
Sub-Freezing Temperatures

Author(s): Rangachary Mukundan
Roger W. Lujan
John R. Davey
Jacob Spendelow
Daniel Hussey
David Jacobson
Muhammad Arif

Intended for: 216th ECS Meeting
Vienna, Austria
October 4-9, 2009



Los Alamos National Laboratory, an affirmative action/equal opportunity employer, is operated by the Los Alamos National Security, LLC for the National Nuclear Security Administration of the U.S. Department of Energy under contract DE-AC52-06NA25396. By acceptance of this article, the publisher recognizes that the U.S. Government retains a nonexclusive, royalty-free license to publish or reproduce the published form of this contribution, or to allow others to do so, for U.S. Government purposes. Los Alamos National Laboratory requests that the publisher identify this article as work performed under the auspices of the U.S. Department of Energy. Los Alamos National Laboratory strongly supports academic freedom and a researcher's right to publish; as an institution, however, the Laboratory does not endorse the viewpoint of a publication or guarantee its technical correctness.

Ice formation in PEM Fuel Cells Operated Isothermally at Sub-Freezing Temperatures

Rangachary Mukundan¹, Roger W. Lujan¹, John R. Davey¹, Jacob S. Spendelow¹, Daniel S. Hussey², David L. Jacobson², Muhammad Arif², and Rodney L. Borup¹

¹Los Alamos National Laboratory, MS D429, MPA-11, Los Alamos, NM 87545

²National Institute of Standards and Technology (NIST), Center for Neutron Research, 100 Bureau Drive, MS 8461, Gaithersburg, MD 20899

The effect of MEA and GDL structure and composition on the performance of single-PEM fuel cells operated isothermally at sub-freezing temperatures is presented. The cell performance and durability are not only dependent on the MEA/GDL materials used but also on their interfaces. When a cell is operated isothermally at sub-freezing temperatures in constant current mode, the water formation due to the current density initially hydrates the membrane/ ionomer and then forms ice in the catalyst layer/GDL. An increase in high frequency resistance was also observed in certain MEAs where there is a possibility of ice formation between the catalyst layer and GDL leading to a loss in contact area. The total water/ice holding capacity for any MEA was lower at lower temperatures and higher current densities. The durability of MEAs subjected to multiple isothermal starts was better for LANL prepared MEAs as compared to commercial MEAs, and cloth GDLs when compared to paper GDLs. The ice formation was monitored using high-resolution neutron radiography and was found to be concentrated near the cathode catalyst layer. However, there was significant ice formation in the GDLs especially at the higher temperature (≈ -10 °C) and lower current density (0.02 A/cm²) operations. These results are consistent with the longer-term durability observations that show more severe degradation at the lower temperatures.

Introduction

The durability of polymer electrolyte membrane (PEM) fuel cells operated at sub-freezing temperatures has received increasing attention in recent years (1). The Department of Energy's PEM fuel cell stack (Automotive application) technical targets for the year 2010 include un-assisted startup from -40 °C and startup from -20 °C ambient in as low as 30 seconds with < 5 MJ energy consumption. Moreover, the sub-freezing operations should not have any impact on achieving the other technical targets including 5000 hours durability.

Literature studies have shown that PEM fuel cell stacks are capable of self-starting from sub-ambient temperatures as low as -10 °C (2) or even -20 °C (3,4) without any external heating. This is primarily achieved by drying out the water in the cell hardware during shutdown, which prevents ice formation from blocking the flow fields during startup (5). Controlled isothermal experiments of single cells have been conducted in the

literature to infer the location of ice formation and to study the performance of fuel cells at sub-freezing temperatures (6-9). These results have all shown that ice formation in the catalyst layer leads to a loss in cell performance and in order to have a successful stack start-up from sub-freezing conditions, it is essential for the stack to heat up above 0 °C before ice formation blocks the electrochemical reaction. Although many groups have reported successful freeze start-ups (3,4), there are very few reported results on the durability of fuel cell stacks that have been subjected to these sub-freezing temperatures. Moreover, there is wide variability in the results reported, with Knights et. al reporting no degradation after 55 sub-freezing starts (5) and Yan et. al. demonstrating significant damage within a few sub-freezing starts on a 25 cm² fuel cell (10). In this paper we explore the effect of MEA and GDL preparation and composition on the freeze durability of single cells.

We have previously characterized the performance of both cloth (E-tek) and paper (SGL) GDLs and reported that the paper GDLs show lower tolerance to sub-freezing temperatures (11). We have also reported the performance of MEAs at -10 °C where ice formation results in mass transport limitations (12). Finally we reported on the effect of MEA preparation on durability and also provided low resolution neutron imaging data to identify ice formation in the land/channel areas (13). In this paper we report the effect of MEA/GDL structure and cell assembly on sub-freezing performance. We also present high-resolution neutron radiographs of single cells operated at sub-freezing temperatures to identify the exact location of ice formation and its effect on durability.

Experimental

Fuel Cell Testing

Several cells were assembled using either LANL prepared or GoreTM Primea[®] Series 57 MEA's and cloth or paper GDLs (14,15). For this study data from 4 different cells, all having a Pt loading of 0.2 mg/cm² at the cathode and 0.1 mg/cm² at the anode, is presented (Table I). Special single cell hardware with cooling loops machined in the end plates was used in order to study the isothermal start-up behavior of 50 cm² cells. The cells were first operated at 0.6 V at 80 °C with air and H₂ at either 100% or 50% inlet RH and 25 psi back pressure. The single cells were then purged using N₂ gas (< 5000 cc/min for < 3 minutes) and cooled down to sub-freezing temperatures. Dry H₂ and dry air were then introduced into the anode and cathode of the cells respectively and their performance was monitored isothermally at various sub-freezing temperatures (-40°C < T < -10°C) at various constant current densities. The voltage and high frequency resistance were monitored during these isothermal operations at sub-freezing temperatures. Cyclic voltammograms (CVs) were obtained before and after the application of current and were used to determine the catalyst surface area available for reaction before and after ice formation. After each operation, the cells were heated back to 80 °C and CVs and polarization curves (VIRs) were obtained under standard conditions in order to track the durability of the cells. Full impedance spectra from 1 kHz to 100 mHz was obtained at the beginning and end of fuel cell operations in order to help identify the various degradation mechanisms (IR, charge transfer and mass transport).

Cell Designation	MEA	Anode and Cathode GDLs	Tests performed
1 (LANL MEA / Cloth GDL)	LANL MEA (Nafion [®] 212)	ELAT GDL : Double sided (Ca), Single sided (An)	5 starts at -10 °C 5 starts at -20 °C 3 starts at -40 °C
2 (LANL MEA / Paper GDL)	LANL MEA (Nafion [®] 112)	SGL GDL : 24 B"C" (5% PTFE in substrate and MPL)	5 starts at -10 °C 5 starts at -20 °C 2 starts at -40 °C
3 (Gore MEA / Cloth GDL)	Gore Primea [®] MESA (18 μm membrane)	ELAT GDL : Double sided (Ca), Single sided (An)	4 starts at -10 °C 4 starts at -20 °C 4 starts at -40 °C
4 (Gore MEA / Paper GDL)	Gore Primea [®] MESA (18 μm membrane)	SGL GDL : 24 B"C" (5% PTFE in substrate and MPL)	7 starts at -10 °C 3 starts at -20 °C 2 starts at -30 °C

Neutron Imaging

Neutron imaging was performed at the NIST Center for Neutron Research (NCNR) on thermal beam tube 2. The measurements were performed using beam #1 and aperture #2 with a fluence rate of 1.9×10^6 neutrons $\text{cm}^{-2} \text{sec}^{-1}$. The imaging was performed using a MCP detector with a resolution of 25 μm and a field of view of 2 cm x 2 cm (16). The MEAs were tested in specially designed hardware with an active area of 2.25 cm^2 to optimize the neutron imaging resolution. Two different hardware, one with a single serpentine flow-channel, and the other with 7 parallel flow channels was tested. The flow channels were machined into gold-coated aluminum end plates that also had cooling loops drilled into it. Two different MEAs were used for this study. The Gore Primea[®] MEA with SGL GDLs was used in the serpentine cell and a Nafion[®] 117 membrane with 6 mg/cm^2 of Pt black on the anode and cathode was used in the parallel cell to better resolve the location of water in the membrane during sub-freezing operations. The cells and the detector were housed in an environmental chamber that was maintained at just above 0 °C and low RH. Once the detector and the chamber reached thermal equilibrium, the cells were operated at 80 °C and 0.6 V, and then dried with N₂ and cooled to sub zero temperatures ($-20 \text{ °C} \leq T < 0 \text{ °C}$) using a chiller that flowed fluid through the cell cooling loops. Once the cell reached thermal equilibrium at the sub-zero temperature of interest, the imaging was started in order to acquire an "initial" image for 15-30 minutes. Then, dry H₂ and air (at 50 cc/min) were introduced into the cell, which was then operated isothermally at constant current till the voltage dropped to zero. The load and the gas flow to the cell was then shut off and a further 15-30 minutes of imaging was performed to obtain the "final" image. The location of ice formation was obtained by referencing the "final" image to the "initial" image. This procedure was necessary since it was difficult to obtain nominally "dry" images without the cell moving during the heating and cooling procedure that was necessary to conduct these sub-zero isothermal experiments. Isothermal sub-freezing experiments were performed at multiple current densities, temperatures, and initial membrane hydration.

Results and Discussion

The performance of the four cells (Table 1) at an operating temperature of $-10\text{ }^{\circ}\text{C}$ is shown in Figure 1. The voltage reaches an OCV of 0.9 V to 1 V on the introduction

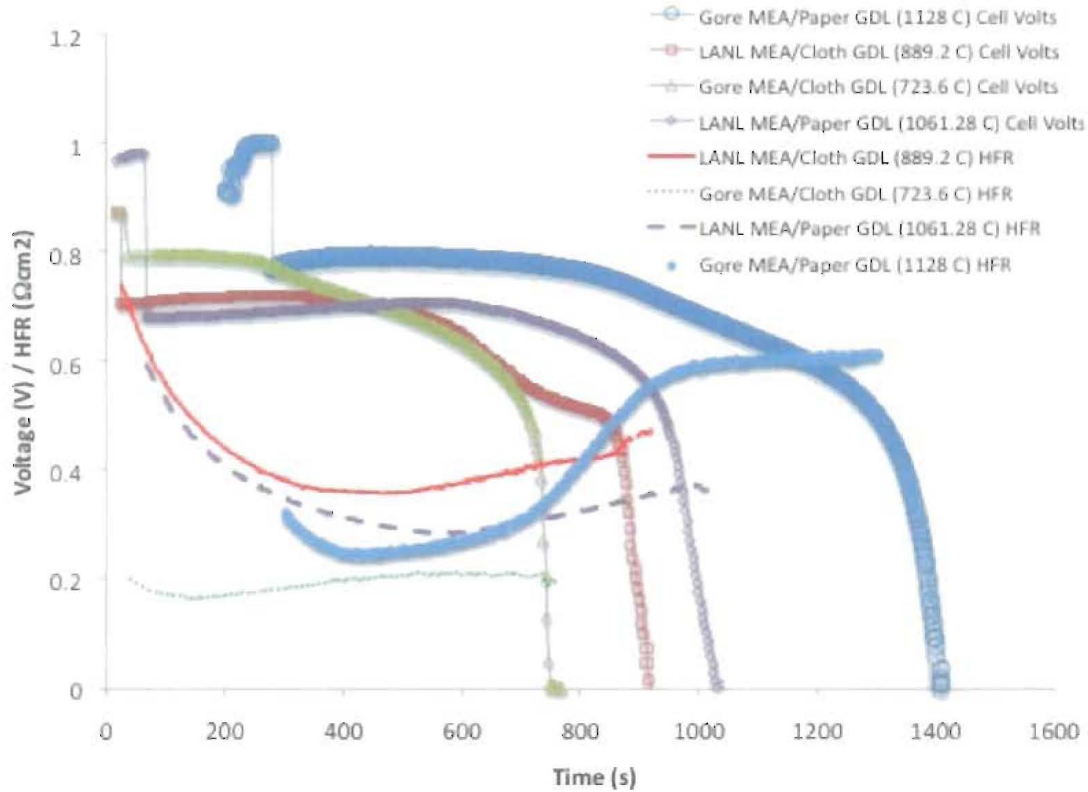


Figure 1. Performance of the cells operated isothermally at $-10\text{ }^{\circ}\text{C}$ and a current density of 0.02 A/cm^2 . The cells were initially operated at $80\text{ }^{\circ}\text{C}$ / 100 % inlet RH / 0.6 V and then dried with N_2 (1 L/min for 2 minutes) and cooled down.

of dry hydrogen and air at 500 cc/min. Once the current of 1 A (0.02 A/cm^2) is applied, the voltage drops to $\approx 0.7\text{ V}$ for the LANL MEA and $\approx 0.8\text{ V}$ for the Gore MEA. This drop is consistent with the larger high frequency resistance (HFR) of the $50\text{ }\mu\text{m}$ thick Nafion[®] membrane in the LANL MEA when compared to the $18\text{ }\mu\text{m}$ thick Gore Select[™] membrane in the Gore MEA. The LANL MEAs show a significant decrease in the HFR indicating that the membrane was not fully hydrated when the cell was started, and the reaction water/ice wets this membrane. The lowest HFR obtained for the LANL MEA corresponded to $0.285\text{ }\Omega\text{cm}^2$ ($\sigma = 0.0175\text{ S/cm}$) and that for the Gore MEA to $0.165\text{ }\Omega\text{cm}^2$ ($\sigma = 0.011\text{ S/cm}$) that is very consistent with the conductivity of fully hydrated Nafion[®] measured at $-10\text{ }^{\circ}\text{C}$ ¹¹ ($\sigma = 0.015\text{ S/cm}$). After the membrane is fully hydrated, the HFR of the cells shows an increase as more and more ice forms and this increase has been correlated previously to water formation under the land area of the cells.¹³ This increase is significant for the Gore MEA with the paper GDL indicating that this MEA/GDL combination does not have good adhesion at the interface and the ice formation tends to open up the contacts thus decreasing the effective contact area and increasing the HFR.

The performance of the LANL MEA/ Cloth GDL cell is illustrated in Fig. 2 where the

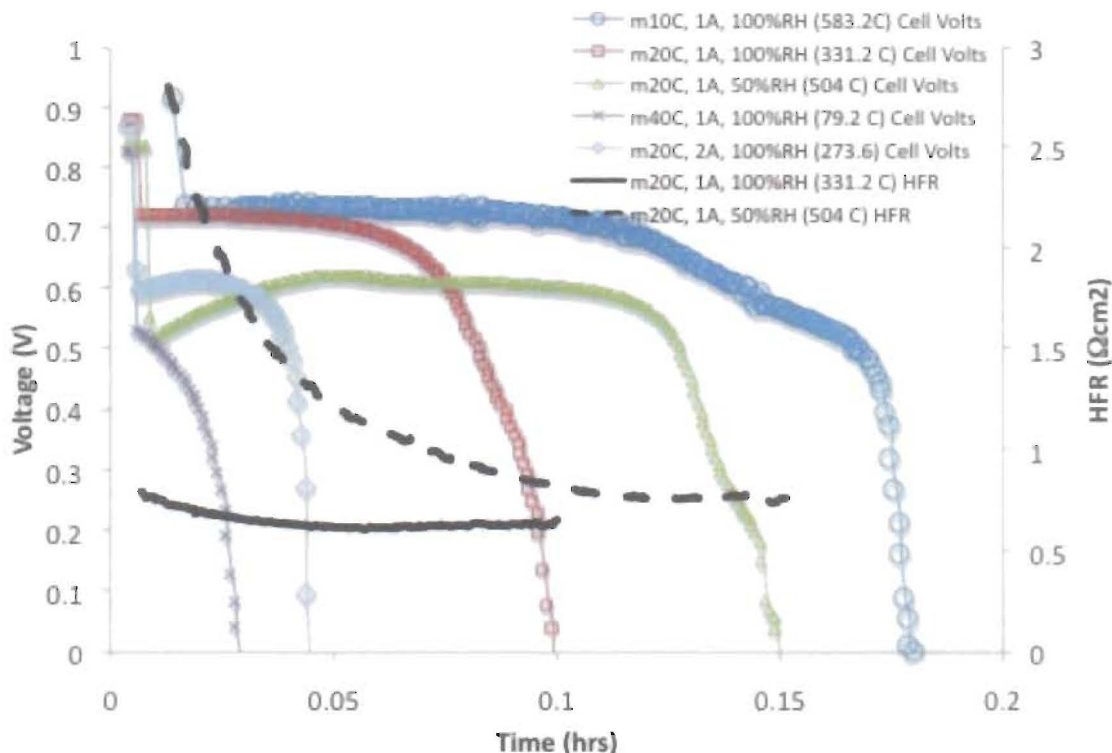


Figure 2. Performance of Cell 1 at various sub-freezing conditions ($-10\text{ }^{\circ}\text{C}$, $-20\text{ }^{\circ}\text{C}$ and $-40\text{ }^{\circ}\text{C}$ and 0.02 and 0.04 A/cm^2) and two initial water contents.

total amount of charge passed through the cell (given in Coulombs in the legend) before the voltage drops to zero indicates the water/ice holding capacity of this cell. It is seen that the water holding capacity decreases with decreasing temperature under similar conditions. For example the cell can hold 1.09 mg/cm^2 of water at $-10\text{ }^{\circ}\text{C}$, 0.62 mg/cm^2 at $-20\text{ }^{\circ}\text{C}$ and only 0.15 mg/cm^2 at $-40\text{ }^{\circ}\text{C}$ when the cell is cooled from a saturated condition and operated at 0.02 A/cm^2 . At a start temperature of $-20\text{ }^{\circ}\text{C}$, the water holding capacity decreases to 0.51 mg/cm^2 when the current density is increased to 0.04 A/cm^2 , or increases to 0.94 mg/cm^2 when the cell is cooled down from a 50% saturated condition. This extra water (when operated from a drier condition) is held in the membrane, which is evidenced by the decrease in HFR from 0.9 to $0.3\text{ }\Omega\text{cm}^2$. If it is assumed that no water is held in the membrane when the membrane is started from a fully saturated condition, the created water of 1.09 mg/cm^2 at $-10\text{ }^{\circ}\text{C}$ and 0.62 mg/cm^2 at $-20\text{ }^{\circ}\text{C}$ is more than what the catalyst layer can hold. For example a $5 - 10\text{ }\mu\text{m}$ catalyst layer with 50% porosity can hold only $0.25 - 0.5\text{ mg/cm}^2$ of water. The extra water/ice is probably stored in the GDL, since the membrane HFR does not decrease indicating a fully saturated membrane.

The durability of the MEAs subjected to the isothermal operations at sub-freezing temperatures was monitored using VIRs, CVs and AC impedance under standard conditions. The VIRs obtained at $80\text{ }^{\circ}\text{C}$, 100% inlet RHs, 25 psig back-pressure, 1.2 stoich H_2 and 2.0 stoich air are presented in Fig. 3. It is seen that there is significant degradation in performance due to the freeze operation. Moreover this degradation is a strong function of the MEA/GDL materials used. The cloth GDL cells showed the least degradation and the paper GDL cells the most. This is consistent with our previous

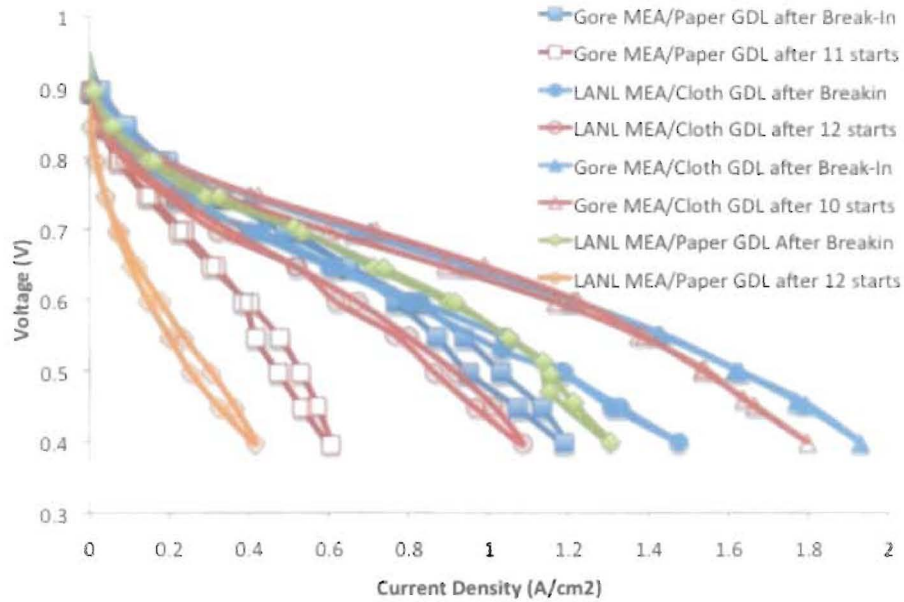


Figure 3. VIR curves of the 4 cells obtained before and after fuel cell testing at sub-freezing temperatures.

results where fiber breakage in the paper GDL lead to performance losses in fuel cells that were frozen *ex situ* repeatedly at $-40\text{ }^{\circ}\text{C}$. The initial performances of the cells were also different with the cloth cells giving better performance (lower HFR) than the paper cells, indicating that cells with better contact resistance or better interfaces result in better durability. In these results the cells were subjected to different sub-freezing starts with cell 1 and cell 2 being subject to 5 starts at $-10\text{ }^{\circ}\text{C}$, and $-20\text{ }^{\circ}\text{C}$, followed by 3 and 2 respectively at $-40\text{ }^{\circ}\text{C}$; cell 3 being subject to 4 starts each at $-10\text{ }^{\circ}\text{C}$, $-20\text{ }^{\circ}\text{C}$ and $-40\text{ }^{\circ}\text{C}$ and cell 4 being subject to 7 starts at $-10\text{ }^{\circ}\text{C}$, 3 at $-20\text{ }^{\circ}\text{C}$, and 2 at $-30\text{ }^{\circ}\text{C}$ (Table I).

In order to better understand this degradation, CVs were performed at various stages during the durability testing. Figure 4 illustrates 3 CVs obtained from cell 1 and show

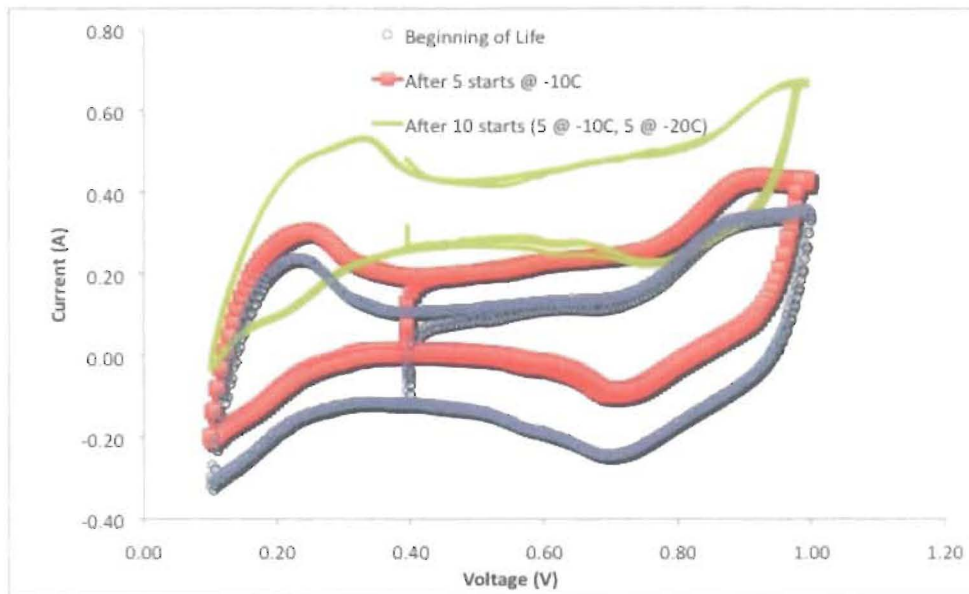


Figure 4. CVs obtained before and after $-10\text{ }^{\circ}\text{C}$ and $-20\text{ }^{\circ}\text{C}$ operation of Cell 1.

that the H₂ cross-over increases with sub-freezing operation. This was observed for both the LANL MEAs (cell 1 and cell 2), while the 2 Gore MEAs (cell 3 and cell 4) showed no such increase in cross-over, even after 12 operations including 4 at -40 °C. This illustrates the importance of the mechanical reinforcement in improving the membrane durability. The Electrochemical surface area (ECSA) measured by integrating the charge under the H₂ adsorption region decreases with multiple starts at sub-freezing temperatures and is shown in Table II. It is seen that the Gore MEAs loose surface area

Table II. ECSA loss for the cells subjected to sub-freeze operation.

Cell Designation	% loss in ECSA after 4 cycles to -10 °C	% loss in ECSA after sub-freezing operations (> 10 starts; see Table I)
1 (LANL MEA / Cloth GDL)	6.8	34.7
2 (LANL MEA / Paper GDL)	8.5	29.7
3 (Gore MEA / Cloth GDL)	27.1	68.6
4 (Gore MEA / Paper GDL)	46	52.8

faster than the LANL MEAs probably due to higher porosity in the catalyst layer (better optimized catalyst layer). This is consistent with the fact that the initial ECSA of the Gore MEAs is \approx 50% greater than those of the LANL MEAs.

AC impedance spectra obtained before and after the sub-freezing operations of cells 1 and 3 is illustrated in Fig 5. It is seen that while there is very little change in the kinetic

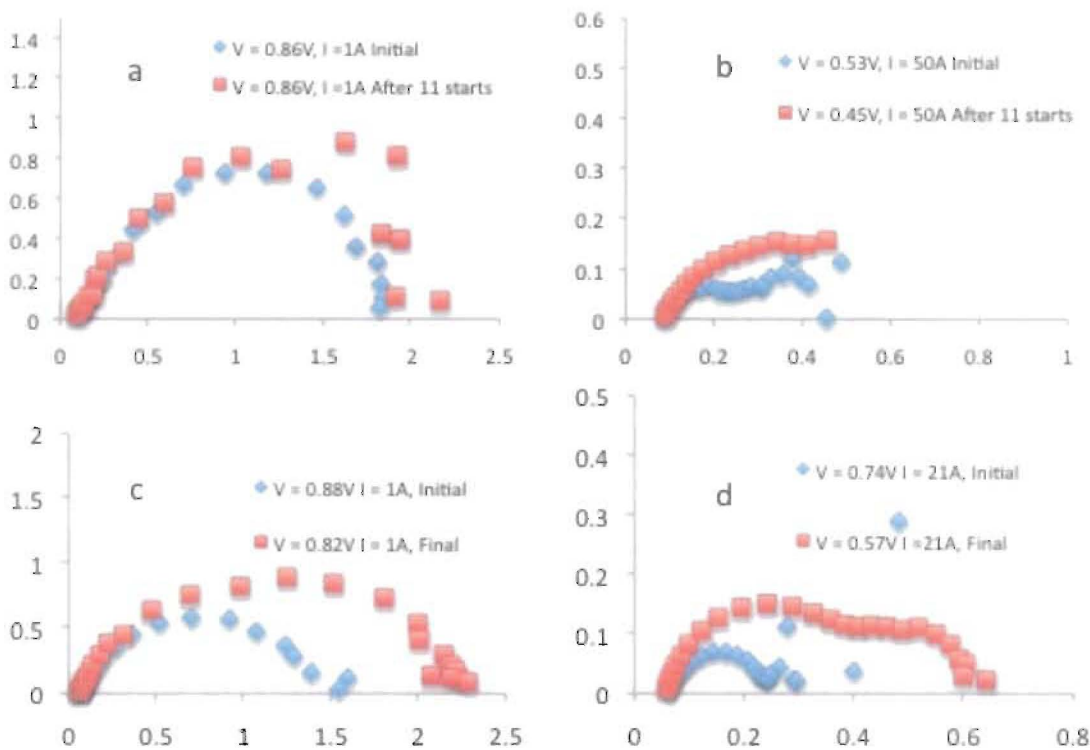


Figure 5. Impedance spectra of cell 1 (a & b) and cell 3 (c & d) showing the charge transfer resistance at low current (a & c) and both the charge and mass transport region at higher current (b & d). The axes are the real and imaginary impedances in Ωcm^2 .

region of the LANL MEA (a), there is significant degradation in the kinetic performance of the Gore MEA (c) that is consistent with the greater loss in ECSA. Although the Gore MEA's initial performance in the kinetic region is far superior to the LANL MEA, this advantage is lost due to the faster degradation of the catalyst layer. The results from the high current density operation (b and d) show that in addition to the degradation in the kinetic region, there is a significant increase in the mass transport resistance as evidenced by the low frequency region of the Nyquist plots. The degradation in mass transport resistance is greater for the paper GDLs than for the cloth GDLs (not shown) indicating that the mass transport resistance is coming from the flooding of the GDL. It should be noted that the paper GDLs used in this study had very low PTFE loadings and would have a tendency to hold more water. Further experiments using more conventional GDLs with loadings up to 23% PTFE in the MPL are planned and are expected to show better durability.

High-resolution neutron imaging performed on specially designed 2.25 cm² hardware with the Gore MEAs and paper GDLs revealed that the ice formation is concentrated in the cathode catalyst layer (Figure 6). Here the peak in the water profiles is at the

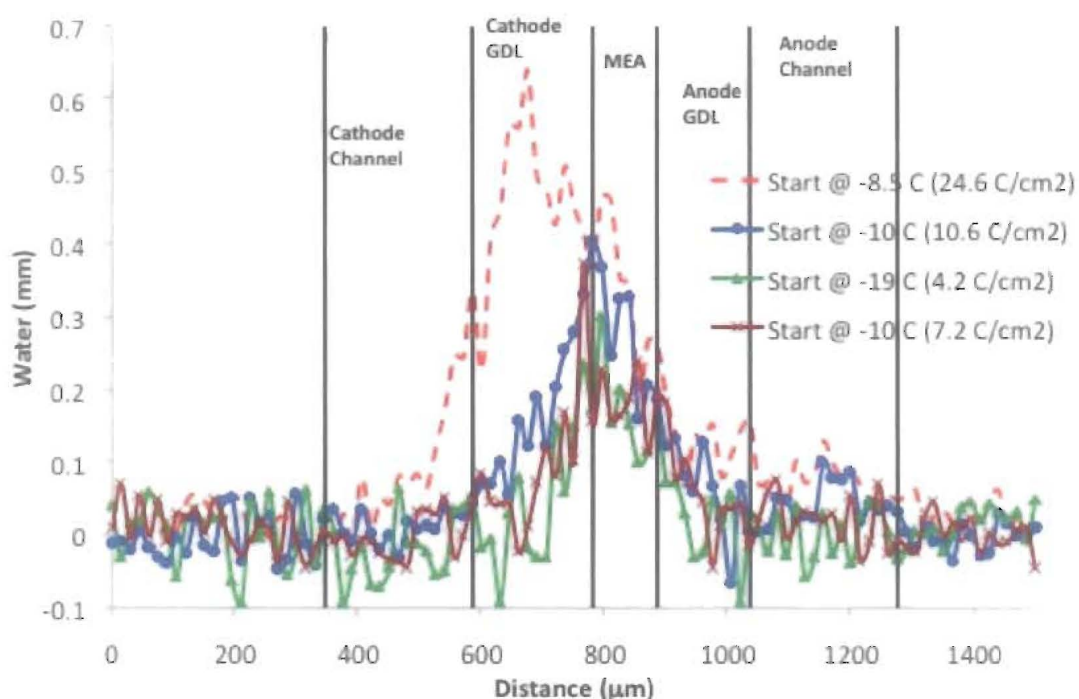


Figure 6. Water/ice profiles obtained after various isothermal sub-freezing operations. The profiles indicate only the ice/water formed due to the current flow at the sub-freezing temperature and are reference to the initial water content before the

MEA/cathode GDL edge for all the isothermal starts where $T \leq -10$ °C. Moreover, the water capacity in these operations is consistent with the standard 50 cm² cell and there is less capacity to hold water at the lower temperatures (0.99 mg/cm² at -10 °C and 0.39 mg/cm² at -19 °C when operated at 0.02 A/cm²) and higher current densities (0.99 mg/cm² at 0.04 A/cm² and 0.67 mg/cm² at 0.12 A/cm² when operated at -10 °C). Moreover when the cell is started from -8.5 °C, the peak in water content is actually well

inside the cathode GDL substrate confirming that there is significant amount of water getting into the GDL before freezing. These results not only help explain the fact that the water holding capacity in these MEAs is greater than that available in the membrane and catalyst layers but also why there is more degradation at the lower temperatures when the ice formation is closer to the catalyst layer. Finally the water/ice profile is also narrower at the higher current densities and lower temperatures, consistent with the lower capacity for ice formation under those conditions.

Preliminary sub-freezing experiments were also performed with a N117 electrolyte in order to better illustrate the water profile by using a thicker membrane. Although these cells did not show comparable performance to the Gore MEAs (their water holding capacity being significantly less), the water profiles shown in Figure 7 are still illustrative

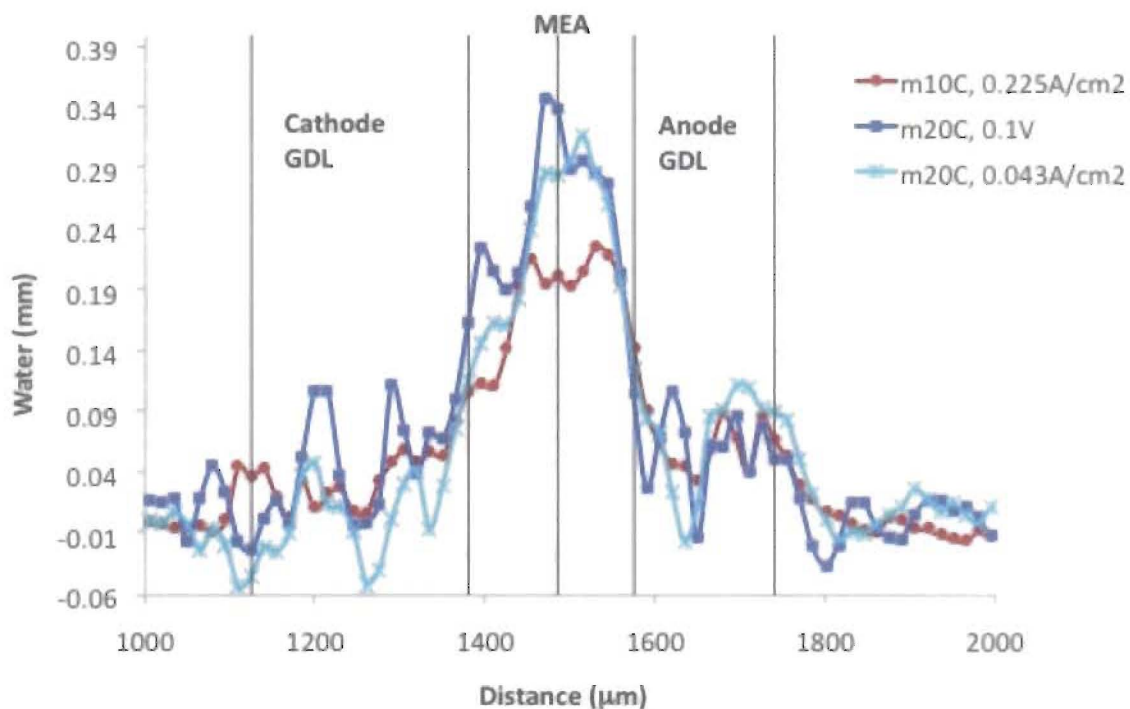


Figure 7. Water/ice profiles obtained after various isothermal sub-freezing operations.

of the ability of the membrane to get hydrated at these temperatures. It is seen that there is a small maxima in water content near the cathode catalyst layer and the rest of the membrane seems to uniformly hydrate as indicated by the flat profile near the middle of the MEA. Further experiments are planned with similar cells with optimized catalyst layers and GDLs that can provide larger water holding capacities and the ability to discern differences within the membrane.

Conclusions

When single PEM fuel cells are subjected to iso-thermal operations at $-10\text{ }^{\circ}\text{C} \leq T \leq -40\text{ }^{\circ}\text{C}$, ice formation results in a loss in voltage at constant current density. The capacity for ice formation in an MEA increases with increasing temperature and decreasing current density. The reaction water initially hydrates the membrane if the membrane is

under-saturated and then forms ice in the cathode catalyst layer/ cathode GDL. In certain MEAs this ice formation resulted in an increasing contact resistance indicating ice formation at the interfaces. This resistance increase was completely recoverable upon heating the cell to above 0 °C and does not appear to result in any longer-term degradation. The total ice formed in a fully hydrated membrane exceeds the capacity of the pore space in the catalyst layer. High-resolution neutron imaging revealed that although the ice distribution is concentrated near the cathode catalyst layer, it extends into the cathode GDL. The extent of ice in the GDL greatly decreases as the start temperature is lowered and/or the current density is increased, indicating that the GDL can be used for water/ice storage only under low current density and higher temperature operations. These results are also consistent with MEA degradation studies that indicate that lower operating temperatures cause much more degradation due to the thermal stresses developed in the catalyst layers. Moreover the degradation was dependent on the MEA and GDL type with the hot pressed MEAs showing better durability than the catalyst coated membranes and the re-inforced membranes showing better durability than the non-reinforced membranes. Finally the paper GDLs tended to show higher degradation rates probably due to ice formation at the GDL/catalyst layer interface or breakage of fibers.

Acknowledgments

This work was supported by the Office of Hydrogen Fuel Cells and Infrastructure Technologies at the U.S. Department of Energy - Energy Efficiency and Renewable Energy. This work was also supported by the U.S. Department of Commerce, the NIST Ionizing Radiation Division, the Director's Office of NIST, the NIST Center for Neutron Research, and the Department of Energy through interagency agreement no. DE-AI01-01EE50660.

References

1. R. Borup, J. Meyers, B. Pivovar, YS. Kim, R. Mukundan et al., *Chemical Reviews*; **107(10)**, 3904 (2007).
2. M. Oszcipok, M. Zedda, D. Riemann, D. Geckeler, *Journal of power sources*, **154**, 404 (2006).
3. *Fuel Cell Operations at Sub-Freezing Temperatures Workshop, Phoenix, Arizona*, http://www1.eere.energy.gov/hydrogenandfuelcells/fc_freeze_workshop.html (2005).
4. Industry PEM Freeze Workshop held at Nuvera, Billerica, Massachusetts, <http://www.nuvera.com/blog/2009/02/26/industry-pem-freeze-workshop-held-at-nuvera/> (2009).
5. S. D. Knights, K. M. Colbow, J. St-Pierre, D. P. Wilkinson, *Journal of power sources*, **127**, 127 (2004).
6. M. Oszcipok, D. Riemann, U. Kronenwett, M. Kreideweis, A. Zedda, *Journal of power sources*, **145**, 407 (2005).
7. E. L. Thompson, J. Horne, W. Gu, H. A. Gasteiger, *J. Electrochem. Soc.*, **155(6)**, B625 (2008).
8. E. L. Thompson, J. Horne, H. A. Gasteiger, *J. Electrochem. Soc.*, **154(8)**, B783 (2007).
9. S. Ge, C. Y. Wang, *J. Electrochem. Soc.*, **154(12)**, B1399 (2007).
10. Q. Yan, H. Toghiani, Y-W Lee, K. Liang, H. Causey, *Journal of Power Sources*, **160**,

1242 (2006).

11. R. Mukundan, Y. S. Kim, F. Garzon, B. Pivovar, *ECS Transactions*, **1(E)**, 403 (2005).
12. R. Mukundan, Y. S. Kim, T. Rockward, J. R. Davey, B. Pivovar, D. Hussey, D. Jacobson, M. Arif, R. Borup, *ECS Transaction*, **11(1)**, 411 (2007).
13. R. Mukundan, J. R. Davey, R. W. Lujan, J. Spendelow, Y. S. Kim, D. Hussey, D. Jacobson, M. Arif, R. Borup, *ECS Transaction*, **16(2)**, 1939 (2008).
14. PRIMEA and GORE are trademarks of W. L. Gore & Associates, Inc.
15. Certain trade names and company products are mentioned in the text or identified in an illustration in order to adequately specify the experimental procedure and equipment used. In no case does such identification imply recommendation or endorsement by the National Institute of Standards and Technology, nor does it imply that the products are necessarily the best available for the purpose.
16. D. S. Hussey, D. L. Jacobson, K. J. Coakley, D. F. Vecchia, and M. Arif, Proceedings of ASME Fuel Cell 2007 Conference, New York, NY (2007).

